DALTON
FULL PAPER

Structure and dynamics of a platinum(II) aminophosphine complex and its nucleobase adducts

Abraha Habtemariam,[a] John A. Parkinson,[a] Nicola Margiotta,[a] Trevor W. Hambley,[b] Simon Parsons[a] and Peter J. Sadler *[a]

[a] *Department of Chemistry, University of Edinburgh, West Mains Road, Edinburgh, UK EH9 3JJ. E-mail: P.J.Sadler@ed.ac.uk*
[b] *School of Chemistry, University of Sydney, NSW 2006, Australia*

Received 21st September 2000, Accepted 1st December 2000
First published as an Advance Article on the web 25th January 2001

The anti-cancer aminophosphine complex, *cis*-[Pt($Me_2N(CH_2)_2PPh_2$-*N*,*P*)Cl($Me_2N(CH_2)_2PPh_2$-*P*)]Cl, **1**, is shown, by ^1H and ^{31}P NMR studies, to undergo reversible chelate ring-closing and -opening in aqueous solution. The rate for this process ($21 \pm 2\ s^{-1}$ at pH* 8.5, 295 K), which is slow on the NMR timescale, varies significantly with pH values, chloride ion concentration and temperature. The chelate-ring-opened form is favoured at acidic pH values. The activation parameters which govern this process, have been determined *via* ^{31}P-2-D EXSY NMR spectroscopy, and the mechanism of chelate ring-opening is discussed. The X-ray crystal structure of the ring-opened complex, *cis*-[Pt($Me_2N(CH_2)_2PPh_2$-*N*,*P*)Cl($Me_2NH(CH_2)_2PPh_2$-*P*)]$(NO_3)_2 \cdot 1.5H_2O$, **1a**, shows that the Pt–N bond is relatively long (2.147 Å). The nucleotide 5′-guanosine monophosphate (5′-GMP) binds *via* N7 and displaces the Cl ligand. Unusually for a platinum(II) amine complex, GMP binding is rapid and reversible. Two isomeric GMP adducts are formed in a 3 : 1 ratio below pH* 6 (pH meter reading in D_2O). Above pH* 8.2, the predominant species are non N7-bound adducts. The on-rate for 5′-GMP binding to the ring-closed form *cis*-[Pt($Me_2N(CH_2)_2PPh_2$-*N*,*P*)$_2$]$^{2+}$, complex **2**, to give the major adduct (pH* 8.5, 298 K) is $0.20\ s^{-1}$ and the off-rate is $0.018\ s^{-1}$. The 5′-GMP adducts were modelled by molecular mechanics calculations. These revealed possible hydrogen bonding between the dangling arm amino group and the 5′-phosphate. Supporting evidence for this came from solution studies with other GMP derivatives (3′, 5′-cyclic GMP, 3′-GMP and 9-ethylguanine). Our findings are discussed in terms of potential new methods for drug delivery and new approaches to drug design.

Introduction

Our interest in platinum(II) aminophosphine complexes arises from their potential anti-cancer activity, in particular their ability to inhibit the growth of cisplatin-resistant cell lines.[1] Chelated bis-aminophosphine metal complexes undergo ring-opening, which can be controlled by factors such as the substituent on the amino nitrogen atom, the length of the N–P linker, the state of protonation of the amino group and the presence of a competing ligand such as chloride. Compounds of this type can exist as a mixture of ring-opened and ring-closed forms. One of our aims is to exploit this behaviour in order to optimise their biological activity. Ring-closed forms may be effective anti-mitochondrial agents since they can be lipophilic cations,[2] whereas ring-opened complexes may bind to specific sites on DNA. There is potential for complexes of this type to act as prodrugs and to be activated at the target site due to local environmental factors such as pH and chloride ion concentration.

Platinum(II) aminophosphine complexes bind to adenine and guanine residues on DNA and can form cross-links between these residues.[3] They can also bind rapidly and strongly to thymine under physiological conditions, in contrast to platinum(II) am(m)ine anti-cancer complexes.[4]

Here we present a detailed study of the influence of temperature, pH and chloride ion concentration on the structure and dynamics of bis(1-*N*,*N*-dimethylamino-2-diphenylphosphinoethane)platinum(II) complexes in aqueous solution. We also show that exchange of the nucleotide, 5′-guanosine monophosphate (5′-GMP) with 5′-GMP bound to the ring-opened complex is relatively rapid on the NMR timescale, which is very unusual for platinum(II) complexes since the Pt–N bonds are usually inert and have a high thermodynamic stability.[5,6] We have used molecular mechanics calculations[7] to shed light on the nature of the isomers formed in guanine nucleotide adducts.

Experimental

Materials and methods

9-Ethylguanine and the sodium salts of 5′-GMP and 3′,5′-cyclic-GMP were purchased from Sigma. The complex *cis*-[Pt($Me_2N(CH_2)_2PPh_2$-*N*,*P*)Cl($Me_2NH(CH_2)_2PPh_2$-*P*)]Cl_2, **1**, was prepared according to previously reported procedures.[8] Reaction of **1** with $AgNO_3$ and subsequent removal of AgCl afforded complex **2**, *cis*-[Pt($Me_2N(CH_2)_2PPh_2$-*N*,*P*)$_2$]-$(NO_3)_2$.

Reaction of 1 with nucleotides. Typically, 0.3 ml of a fresh solution of 40 mM **1** or **2** in D_2O was mixed with 0.3 ml of a 40 mM solution of the appropriate nucleotide in D_2O in a 5 mm NMR tube. The pH* was adjusted to the desired value with either DNO_3 or NaOD.

pH Measurements. A Corning 145 pH meter, equipped with a micro-combination electrode (Aldrich) calibrated with standard buffer solutions at pH 4 and 7, was used for all pH measurements. The pH readings for D_2O solutions are designated as pH* values, and are uncorrected for the effect of deuterium on the glass electrode.

Calculations of p*K* values. The pH titration curves were fitted to the Henderson–Hasselbalch equation using the program KALEIDAGRAPH.[9]

 DOI: 10.1039/b007670h

Table 1 Crystallographic data for *cis*-[Pt($Me_2N(CH_2)_2PPh_2$-*N*,*P*)Cl($Me_2NH(CH_2)_2PPh_2$-*P*)]$(NO_3)_2$·1,5H_2O (**1a**)

	1a
Formula	$C_{32}H_{44}ClN_4O_{7.5}P_2Pt$
M	897.19
Temperature/K	150
Crystal system	Monoclinic
Space group	$P2_1/n$
λ/Å	0.71073
a/Å	12.009(3)
b/Å	12.415(3)
c/Å	24.278(5)
β/°	91.74(2)
U/Å^3	3618.0(13)
Z	4
D_c/g cm^{-3}	1.647
μ(Mo-Kα)/mm^{-1}	4.092
F(000)	1796
Crystal size/mm^3	0.12 × 0.16 × 0.27
Data/restraints	6392/30
Parameters	424
Goodness of fit on F^2	1.041
Colour, habit	Colourless, block
Reflections collected	6393
*wR*2 indices (F^2)	0.08974
Conventional $R[F > 4\sigma(F)]$	*R*1 = 0.0400 [4953 data]
ρ_{min}, ρ_{max}/e Å^{-3}	−0.56, 1.24

X-Ray crystallography

Crystals suitable for X-ray analysis were obtained from an aqueous solution of complex **1** which gave rise to the nitrate salt, *cis*-[Pt($Me_2N(CH_2)_2PPh_2$-*N*,*P*)Cl($Me_2NH(CH_2)_2PPh_2$-*P*)]-$(NO_3)_2$·1.5H_2O, **1a**, under low pH conditions (the pH of the solution was lowered by addition of HNO_3). Crystal data and other experimental details are summarised in Table 1. The crystal was handled under perfluoropolyether oil, and data were collected on a Stoë Stadi-4 diffractometer equipped with an Oxford Cryosystems low-temperature device. A numerical absorption correction was applied by Gaussian integration after refinement of the crystal dimensions against a set of ψ-scans (transmission range 0.664–0.855).[10] Data were measured to $2\theta_{max}$ = 50° in ω–θ mode with on-line profile fitting.[11] The structure was solved by Patterson methods[12] and completed by iterative cycles of least-squares refinement and difference Fourier syntheses.[13] One of the nitrate anions is disordered over two sites with equal occupancies (0.5); in one of these, the anion appears to be H-bonded to a partial-weight water molecule which occupies the site of the alternative anion position. All major residual density lies in this region, suggesting further unresolved disorder. The partial weight nitrates were restrained to be geometrically similar to each other and to have three-fold symmetry. All full-weight non-H atoms were refined with anisotropic displacement parameters; H-atoms attached to C or N were placed geometrically and allowed to ride on their parent atoms.

CCDC reference number 186/2301.

See http://www.rsc.org/suppdata/dt/b0/b007670h/ for crystallographic files in .cif format.

NMR spectroscopy

One-dimensional (1-D) NMR spectroscopy. Standard 1-D NMR spectra were acquired at 298 K using Jeol GSX 270 (^{1}H, 270 MHz; ^{31}P, 109.67 MHz), Bruker DRX500 and DMX500 (^{1}H, 500 MHz; ^{31}P, 202 MHz) and Varian ^{UNITY}*INOVA* 600 (^{1}H, 600 MHz) NMR spectrometers. Typically ^{1}H 1-D NMR spectra were acquired with 64–256 transients using a pulse width of 45–60° into 16–32 K data points with a relaxation delay of 2–3 s. The final digital resolution of the data was 0.2 Hz/point. The residual HOD resonance from the solvent was suppressed by presaturation. Similarly, standard ^{31}P-{^{1}H} 1-D NMR spectra were acquired with 512–2048 transients using inverse-gated decoupling into 16–32 K data points with a relaxation delay of 0.2 s. The final digital resolution of the data was 3–5 Hz/point. Particular attention was given to the acquisition of ^{31}P-{^{1}H} 1-D NMR data at 202 MHz under conditions suitable for the accurate measurement of integrals. Data were acquired over a spectral width of 40.65 kHz into 41662 data points (acquisition time = 512 ms) using a 90° pulse (24 μs) followed by a recycle delay of 10.0 s to allow for full recovery of ^{31}P magnetization.

^{31}P T_1 Relaxation measurements. ^{31}P T_1 Relaxation times were measured using the standard inversion-recovery sequence (180°–t_1–90°–acquire) in which t_1 was varied from 100 ms to 10 s. Proton decoupling was applied during the acquisition period. Data were Fourier-transformed into 2 K data points using a 2 Hz line broadening function. Relaxation times were calculated using the T_1 routine within Xwin-nmr (version 1.3, Bruker Ltd.).

Two-dimensional (2-D) NMR spectroscopy. For studies of chelate ring-opening, 2-D ^{31}P–^{31}P EXSY NMR data sets were acquired with ^{1}H decoupling using the pulse sequence 90°–t_1–90°–*mix*–90°–acq where t_1 is the incremental delay and *mix* is the period during which chemical exchange can occur. All 2-D data sets were acquired at 202 MHz in a phase-sensitive mode using the TPPI scheme; 16 transients were acquired into 1024 data points for each of 128 t_1 increments over ω_1 and ω_2 frequency widths of 16.2 kHz. A recycle delay of 10.0 s allowed for full recovery of ^{31}P magnetization between transients. A total of 64 dummy transients were included to achieve a steady state prior to the acquisition of data. All 2-D data sets were processed with identical parameters. Data in ω_2 were apodized using a 90° shifted sinebell-squared window function prior to Fourier transformation. Data in ω_1 were apodized using the same window function and zero-filled once to 256 data points prior to Fourier transformation. The transformed data were phase- and base-plane-corrected prior to volume integration. All ^{31}P NMR data sets were referenced externally to 85% H_3PO_4 (in H_2O) at 0 ppm. Both 1-D and 2-D NMR data sets were acquired at various pH values, temperatures and mixing times (see text for details). Probe temperatures were calibrated using methanol and ethylene glycol samples. All NMR data acquisition and processing was carried out using Xwin-nmr (version 1.3, Bruker Ltd.). 2-D ^{1}H ge-COSY45, TOCSY and NOESY NMR data sets were acquired at 600 MHz on *cis*-[Pt(5′-GMP-N7)($Me_2N(CH_2)_2PPh_2$-*N*,*P*)($Me_2NH(CH_2)_2PPh_2$-*P*)]$^{3+}$ (charge on GMP is ignored in formulae in this paper) in the absence of chloride ions. Magnitude mode 2-D ge-COSY45 data were acquired with 8 transients into 4096 complex data points (acquisition time = 410 ms) over a 5 kHz spectral width in both dimensions for each of 1024 t_1 increments (200 ms acquisition time in ω_1). Phase-sensitive 2-D TOCSY data were acquired with 8 transients into 4096 complex data points (acquisition time = 410 ms) over a 5 kHz spectral width in both dimensions for each of 2 × 512 hypercomplex t_1 increments. A mixing time of 50 ms was applied using an MLEV17 spin-lock field. Phase-sensitive 2-D NOESY data (mixing time 150 ms) were acquired with 8 transients into 2048 complex data points (acquisition time = 145 ms) over a 7 kHz spectral width in both dimensions for each of 2 × 512 hypercomplex t_1 increments, using a recycle delay of 3.5 s. Data from NOESY experiments were used to generate inter-proton distance constraints where appropriate. ^3J coupling constants were measured directly from 1-D ^{1}H and ^{1}H-{^{31}P} data sets and were used to define dihedral angle constraints for modelling studies.

Adducts formed between **1** or **2** and the nucleotide 5′-GMP were also studied by ^{1}H–^{1}H 2-D EXSY NMR spectroscopy at 600 MHz. For each of 2 × 512 hypercomplex t_1 increments,[14] 32 transients were acquired into 2048 complex data points over a

spectral width of 6 kHz in both dimensions. Data sets were acquired at temperatures of 288, 298, 308, 318 and 328 K. Mixing times of 50, 100, 150, 200, 250, 300, 400, 500 and 1000 ms were used to assess the build-up of exchange peaks for the purposes of establishing suitable conditions for the calculation of exchange rates. Relative integrals of diagonal and off-diagonal peaks were measured by volume integration of the data. The population matrices P for the various species were calculated from integration of 1-D ^{1}H NMR spectra. Rate constants were extracted from the appropriate off-diagonal elements of the computed kinetic matrix L. Data were processed using VNMR (version 4.1, Varian Instruments Ltd.) or Xwin-nmr (version 1.3, Bruker Ltd.).

Populations of complexes of **1** and **2** in solution were determined by integration of baseline-corrected 1-D ^{31}P-{^{1}H} NMR spectra acquired under different conditions of pH and temperature. Error limits were derived from the differences in integrals of the two separate ^{31}P signals arising from the ring-opened form of the complex. Integrals from 2-D NMR spectra were used for exchange rate calculations. Volume integrals were measured only for ^{31}P bound to $I = 0$ (central peak 66% of Pt). Volumes from peaks on opposite sides of the diagonal were averaged. Species populations for the nucleotide-complexes were measured according to a similar procedure with data acquired at 600 MHz using the H8 resonance from the nucleotide base.

Analysis of chelate ring-opening dynamics. Exchange rates were calculated using the program D2DNMR[15] and two-, three- or four-site models. Volume integrals and population estimates were used as input parameters. Error limits were based on variations in integrals and are compared with the output from the exchange rate program. Variations in rates within an exchange rate matrix were of the same order as errors calculated directly using D2DNMR. Bandshape analysis was carried out using the program gNMR[16] using a ^{31}P-{^{1}H} linewidth of 7.0 Hz, a $^2J(^{31}P–^{31}P)$ coupling constant of 17 Hz and by variation of the exchange rate parameters.

Calculation of activation parameters. Thermodynamic calculations were made on the basis of the exchange rate data using the fitting program KALEIDAGRAPH.[9] The data for complexes **1** and **2** over the temperature range 276–301 K were fitted to the Arrhenius relationship (eqn. 1):

$$\ln k_{ex} = -\frac{E_a}{RT} + \ln A \qquad (1)$$

where k_{ex} is exchange rate (s^{-1}), E_a is activation energy (J mol^{-1}), $R = 8.31441$ J K^{-1} mol^{-1}, T is absolute temperature (K), and A is the frequency factor. Activation parameters $\Delta G^‡$, $\Delta H^‡$ and $\Delta S^‡$ derived for these exchange processes were calculated using eqn. 2.[17]

$$\log_{10}\left(\frac{k_{ex}}{T}\right) = 10.318 - \frac{\Delta H^‡}{19.143T} + \frac{\Delta S^‡}{19.143} \qquad (2)$$

Molecular modelling

Starting models were generated using the program HyperChem[18] and energy-minimised using the MOMECSGI[19] program with a force field based on one described elsewhere.[20] New parameters were required for the phosphine donor groups and were based on those for thioether donor groups and adjusted to reproduce the geometry of **1**. All models were energy minimised using MOMECSGI until convergence was achieved. Energy profiles associated with rotation about the Pt-N7 coordination bond were generated by applying constraints[21] to a torsion angle about this bond and stepping through the angles corresponding to conversion from one orientation to the other.

Table 2 Selected bond distances (Å) and bond angles (°) for *cis*-[Pt($Me_2N(CH_2)_2PPh_2$-*N*,*P*)Cl($Me_2NH(CH_2)_2PPh_2$-*P*)][NO_3)$_2$·1.5H_2O (**1a**)

Pt(1)–N(4A)	2.147(5)
Pt(1)–P(1A)	2.2311(17)
Pt(1)–P(1B)	2.2597(18)
Pt(1)–Cl(1)	2.3737(16)
N(4A)–Pt(1)–P(1A)	84.54(15)
N(4A)–Pt(1)–P(1B)	175.43(14)
P(1A)–Pt(1)–P(1B)	99.63(6)
N(4A)–Pt(1)–Cl(1)	90.06(15)
P(1A)–Pt(1)–Cl(1)	172.90(6)
P(1B)–Pt(1)–Cl(1)	85.63(6)

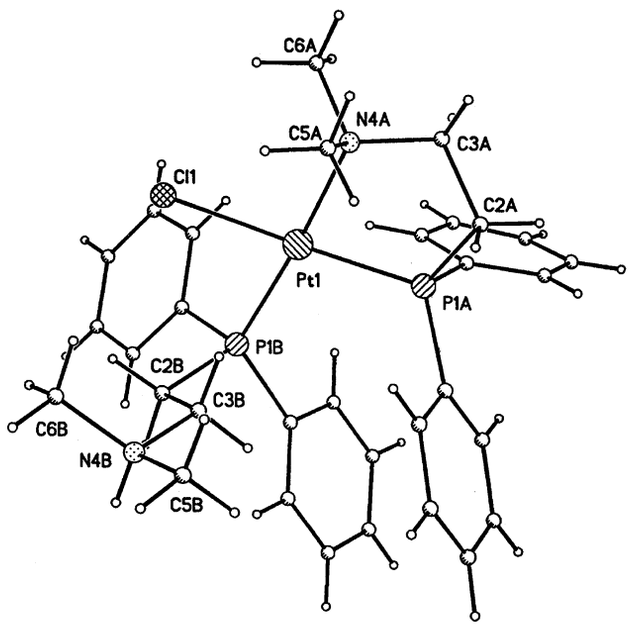

Fig. 1 X-Ray crystal structure of the cation of *cis*-[Pt($Me_2N(CH_2)_2PPh_2$-*N*,*P*)Cl($Me_2NH(CH_2)_2PPh_2$-*P*)][NO_3)$_2$·1.5H_2O (**1a**) showing one closed P,N chelate ring and one protonated dangling arm.

Results

X-Ray crystal structure of complex 1a

Crystals of the protonated, ring-opened complex, *cis*-[Pt($Me_2N(CH_2)_2PPh_2$-*N*,*P*)Cl($Me_2NH(CH_2)_2PPh_2$-*P*)][NO_3)$_2$·1.5H_2O, **1a**, suitable for X-ray analysis were obtained from aqueous solution at pH 2.5. The X-ray crystal structure is shown in Fig. 1 and selected bond distances and angles are listed in Table 2. Platinum(II) in the complex is square-planar and coordinated to N, Cl and the two P atoms in a *cis* arrangement. The large P(1A)–Pt(1)–P(1B) angle (99.63°) can be attributed to steric interactions of the phenyl substituents on P. This is also reflected in the reduction of the P(1A)–Pt–N(4A) angle to 84.5°. The Pt–Cl distance (2.374 Å) is as expected for Cl *trans* to phosphorus.[22] The two Pt–P distances are relatively short,[23] with that *trans* to Cl (2.231 Å) being somewhat shorter than that *trans* to N (2.260 Å). The Pt–N bond distance (2.147 Å) is significantly longer than those observed for the related ring-closed complex *cis*-[Pt($H_2N(CH_2)_2PPh_2$-*P*,*N*)$_2$]Cl_2 (2.090, 2.111 Å),[24] which does not have substituents on N.

Dynamics of chelate ring-opening and -closing

1-D ^{31}P-{^{1}H} and 2-D ^{31}P–^{31}P–{^{1}H} EXSY NMR spectra of an aqueous solution containing a mixture of the ring-opened complex **1** and ring-closed form **2** of the aminophosphine complex (Scheme 1, processes not involving 5′-GMP) are shown in Fig. 2. The 2-D NMR data are characterized by the following features: (i) 3 peaks along the diagonal (**a**, **b** and **c**); (ii) off-diagonal exchange cross-peaks (linked by solid lines in Fig. 2);

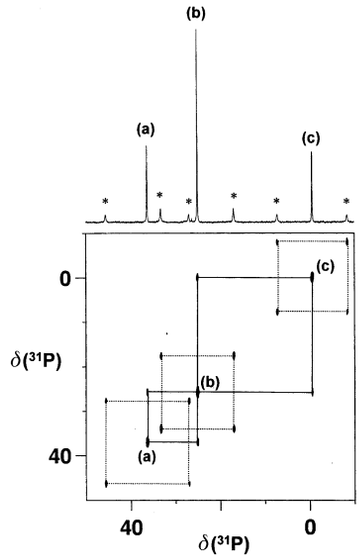

Fig. 2 Top, 202 MHz 1-D ^{31}P-{^{1}H} NMR spectrum of a 40 mM solution of *cis*-[Pt($Me_2N(CH_2)_2PPh_2$-*N*,*P*)Cl($Me_2NH(CH_2)_2PPh_2$-*P*)]Cl_2 **1** in D_2O, pH* 7, 277 K, showing peaks **a** and **c** for the ring-opened complex **1** as well as peak **b** for the ring-closed complex **2**. ^{195}Pt satellites are marked with asterisks (*). See Scheme 1 for assignments. Bottom, 2-D ^{31}P–^{31}P-{^{1}H}-EXSY NMR spectrum (mixing time 7.5 ms) of the same solution. Solid lines link the exchange cross peaks.

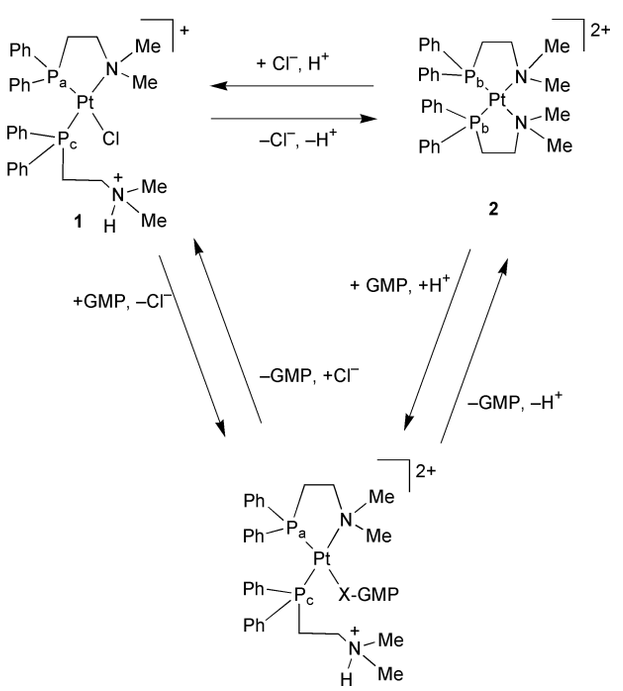

Scheme 1 X = N7 (**3**/**3***), X = N1 (**4**).

(iii) sets of ^{195}Pt–^{31}P satellite signals (see Fig. 2). The diagonal peaks **a** and **c** correspond to two ^{31}P NMR resonances from the chelate ring-opened form of the complex, **1**, in which the ^{31}P atoms are non-equivalent. Resonance **a** is assigned to P in the P,N chelate ring (P_a, Scheme 1) of the ring-opened complex, **1** (δ 36.3, $^{1}J(^{195}Pt–^{31}P)$ = 3767 Hz). The high frequency shift of peak **a** is consistent with its presence in a 5-membered chelate-ring[25] and its associated $^{1}J(^{195}Pt–^{31}P)$ coupling constant is typical of ^{31}P *trans* to Cl.[26] Resonance **c** is assigned to P of the pendant arm ligand (P_c, Scheme 1) of complex **1** (δ −0.55, $^{1}J(^{195}Pt–^{31}P)$ = 3160 Hz). Its $^{1}J(^{195}Pt–^{31}P)$ coupling constant is typical of ^{31}P *trans* to N.[26] The singlet **b** (δ 25.1, $^{1}J(^{195}Pt–^{31}P)$ = 3292 Hz) is assigned to the two equivalent ^{31}P nuclei (P_b, Scheme 1) of the chelate ring-closed complex, **2**. The off-diagonal exchange

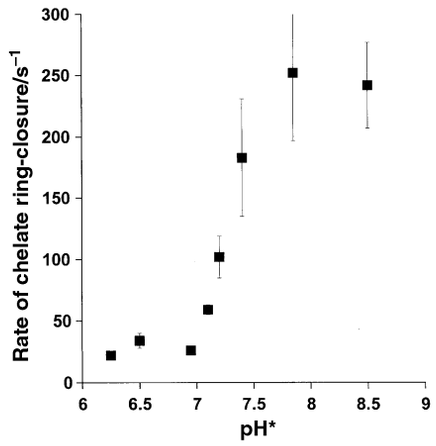

Fig. 3 Variation of the rate of ring-closure of complex **1** (20 mM, 295 K) with pH* (Scheme 1).

cross-peaks, arise from the dynamic process of chelate ring-opening and closing, which results in chemical exchange of the ^{31}P atoms (*vide infra*).

The pH dependence of the rate of chelate ring-closure was studied by titrating a 20 mM aqueous solution of complex **1** with DNO_3 (pH* range 6.0–9.0; 295 K). Rates were determined from 2-D ^{31}P EXSY NMR data. A plot of chelate ring-closure rate *vs.* pH* is shown in Fig. 3. At high pH (> 8.5) the chelate ring-closed form of the complex, **2**, was dominant (74%). The corresponding rate of ring-closure was relatively high (242 ± 35 s^{-1} at 295 K, pH* 8.5). There was a reduction in the rate of chelate ring-closure with decreasing pH* to the point where, at pH* 5.5, this rate was negligibly small. In contrast, even at very high pH, the chelate ring-closed species was never present to more than 80% of the total amount of complex. The pH dependences of the rates of chelate ring-opening and ring-closure were also measured as a function of temperature over the range 276–301 K. At pH* 8.5, the chelate ring-closing process was dominant, especially at higher temperatures, when the exchange rate for chelate ring-closure was an order of magnitude higher than the rate of chelate ring-opening (*e.g.* 242 ± 35 s^{-1} compared with 21 ± 2 s^{-1} for chelate ring-opening at 295 K). In comparison, at pH* 7.1 the rate of chelate ring-closure was much lower (59 ± 4 s^{-1} at 295 K) while the rate of chelate ring-opening showed a small increase (31 ± 2 s^{-1} at 295 K). At pH* 6.25 and 295 K, the rates of chelate ring-opening (30 ± 2 s^{-1}) and chelate ring-closure (22 ± 2 s^{-1}) were similar. Thermodynamic calculations were made on the basis of the exchange rate data derived from 2-D ^{31}P–^{31}P EXSY NMR studies. The $\Delta G^{\ddagger}$, $\Delta H^{\ddagger}$ and $\Delta S^{\ddagger}$ values derived for the exchange processes shown in part of Scheme 1 are given in Table 3.

The exchange processes between **1** and **2**, shown in Scheme 1 influenced the line-shapes of peaks in ^{31}P-{^{1}H} NMR spectra acquired at different temperatures. Raising the sample temperature led to signal broadening. Simulations were carried out for low pH conditions, when the exchange rates were slow enough to allow the $^{2}J(^{31}P–^{31}P)$ splitting (*ca.* 17 Hz) to be observed. The results compare well with those derived from the 2-D NMR studies described above. Good fits were obtained when the exchange rate-constants derived from the D2DNMR analysis were used for the band-shape analysis. This confirmed the experimental results and cross-validated both methods used for calculating the exchange rates of the chelate ring-opening and -closing processes.

Chloride ion dependence. Reaction of **1** with $AgNO_3$ afforded complex **2**, which was subsequently titrated with chloride (pH* 8.5, 295 K). 2-D ^{31}P EXSY NMR data were acquired at different stages of the chloride ion titration. These were used to calculate the rates of chelate ring-opening. The results are

Table 3 Activation parameters for chelate ring-opening and -closure processes

pH*	Process[a]	ln A	$E_a^{\ddagger}$/kJ mol^{-1}	$\Delta H^{\ddagger}$/kJ mol^{-1}	$\Delta S^{\ddagger}$/J mol^{-1} K^{-1}	$\Delta G^{\ddagger}$/kJ mol^{-1}
8.5	C	17 ± 2	33 ± 5	46 ± 3	−42 ± 12	59 ± 6
	O	25 ± 1	49 ± 3	31 ± 1	−114 ± 17	64 ± 5
7.1	C	21.4 ± 0.1	42.6 ± 0.2	40.23 ± 0.15	−75 ± 1	62.3 ± 0.4
	O	18.5 ± 0.3	37 ± 0.6	34.6 ± 0.6	−99 ± 3	63.2 ± 1.5
6.25	C	16.7 ± 0.4	33.5 ± 0.7	31.05 ± 0.75	−114 ± 3	63.9 ± 1.6
	O	16.8 ± 0.4	32.7 ± 0.8	30.4 ± 0.8	−113 ± 3	63.1 ± 1.7

[a] C = Chelate ring-closing, O = chelate ring-opening.

Table 4 δ (^{31}P) and $^1J(^{195}\text{Pt}–^{31}\text{P})$ coupling constants (Hz) for nucleobase adducts of complexes **1** and **2**

Adduct	δ (^{31}P) P,N Chelate-ring		Pendant-arm		Nucleotide-phosphate		^1J(Pt,P)	^2J(P,P)	Isomer-ratio	pH*
5′-GMP	26.41[a]	27.10[b]	−7.70[a]	−6.67[b]	2.28[a]	1.82[b]	3468,[c] 3203[d]	20	3:1	5.06
3′-GMP	28.73	29.00	−4.87	−5.15	1.21	1.08	3495,[c] 3201[d]	20	1:1	5.00
9-ethylguanine	30.98		−1.32		—	—	3471,[c] 3142[d]	21	[e]	5.60
3′,5′-Cyclic GMP	28.66[a]	28.94[b]	−4.78[a]	−5.06[b]	—	—	3483,[c] 3196[d]	21	1.1:1	5.10

[a] Major adduct. [b] Minor adduct. [c] *trans* to N7. [d] *trans* to chelate-ring N. [e] Only one isomer observed.

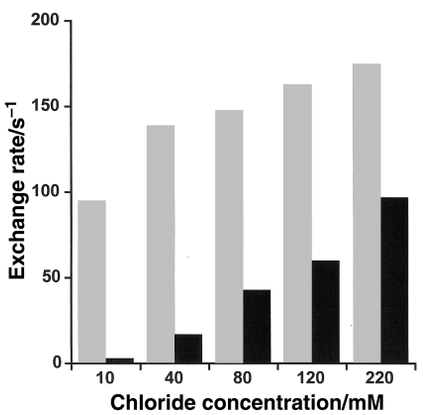

Fig. 4 Dependence of chelate ring-closure (grey) and ring-opening (black) rates on chloride concentration for complexes **1** and **2**, respectively. Conditions: 40 mM **1** + **2**, pH* 8.5, 298 K.

shown in Fig. 4. The rates of chelate ring-opening and closing increased with increasing chloride ion concentration.

Binding of 1 to 5′-GMP

When an equimolar quantity of 5′-GMP was added to an aqueous solution of **1** and monitored using both ^{1}H and ^{31}P-{^{1}H} NMR spectroscopy (293 K, pH* 5.5), the reaction was complete within 5 minutes. The H8 singlet ^{1}H NMR resonance of free 5′-GMP (δ 8.10) almost disappeared, while two new singlets appeared to higher frequency at δ 9.31 and δ 9.12. The new resonances suggested the formation of two 5′-GMP adducts in a 3:1 ratio, corresponding to major and minor adducts (**3** and **3***), respectively. The high-frequency shift of these H8 ^{1}H NMR resonances compared with that of free 5′-GMP is typical of metal coordination through the N7 atom of guanine.[27] Above pH* 6.5, an additional H8 resonance appeared (δ 8.10), which may be assignable to an N1 bound adduct, **4** (*vide infra*). The ^{31}P-{^{1}H} NMR spectrum at pH* 5.5 also showed new sets of major and minor resonances corresponding to the presence of **3** and **3***. These resonances appeared in three groups: (a) two sharp doublets assignable to P in *P*,*N* chelate rings; (b) two broad doublets assignable to P in P-bound chelate ring-opened ligands; (c) two singlets arising from the phosphate groups of coordinated 5′-GMP. Chemical shift and coupling constant data associated with each of these adducts are given in Table 4. The similarities of the NMR

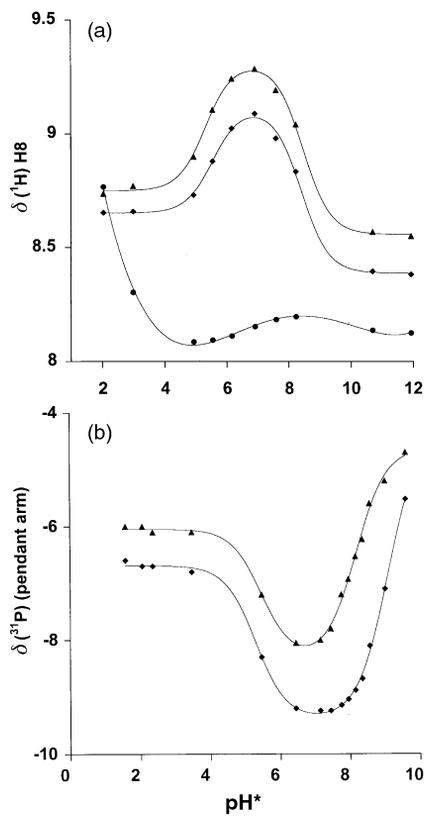

Fig. 5 (a) pH* dependence of the chemical shift of the H8 ^{1}H NMR peak of 5′-GMP in complex **3** (▲), **3*** (◆) and free 5′-GMP (●) at 298 K, showing the lack of protonation of N7 for **3**/**3*** at low pH* and deprotonation of N1 and phosphate at higher pH*. The corresponding pK_{a1} values were 5.31 (**3**) and 5.49 (**3***) (attributed to protonation of the phosphate group of 5′-GMP) and 8.51 (**3**) and 8.43 (**3***) (associated with deprotonation of N1 of 5′-GMP). (b) Dependence of the chemical shift of the P atom of the pendant arm with pH* for **3** (▲) and **3*** (◆). The corresponding pK_{a1} values were 5.29 (**3**) and 5.46 (**3***), respectively. Above pH* 9, data were incomplete and not fitted due to resonance broadening.

parameters for **3** and **3*** suggest that they are very similar adducts, perhaps isomers.

The binding of 5′-GMP through N7 was further confirmed by a pH titration of **3**/**3*** (Scheme 1). For free 5′-GMP, protonation at N1 (pK_a = 9.7) and N7 (pK_a = 2.4) is known to shift the H8 ^{1}H NMR resonance to higher frequency. In

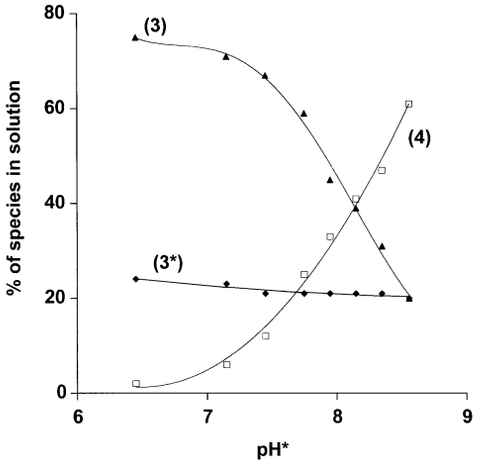

Fig. 6 The relative populations of all the species formed from reaction of equimolar amounts of **2** and 5′-GMP as a function of pH*: **3** (▲), **3*** (◆) and **4** (□).

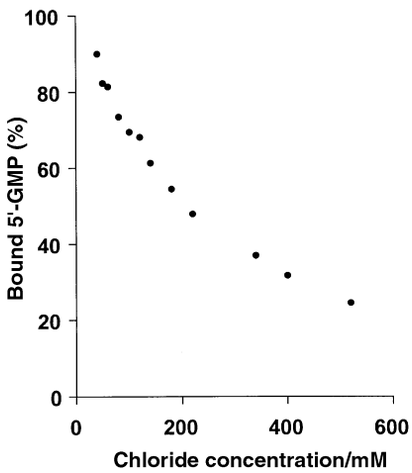

Fig. 7 Displacement of 5′-GMP from complex **3/3*** on addition of various amounts of Cl^- as determined by ^{31}P NMR. Conditions: 20 mM of complex (in D_2O), pH* 8.5, 298 K.

contrast, phosphate protonation ($pK_a = 6.2$ and ≤ 1) causes chemical shift changes to low frequency.[28,29] Over the pH* range 2.4–11.5, **3** and **3*** were found to be stable (Fig. 5a), although the corresponding ratios of the major and minor isomers varied (from 3 : 1 at pH* 5.5 to 1 : 1 at pH* 8.5; Fig. 6). No change in the chemical shift of H8 was observed over the pH* range 2–4, confirming the binding of platinum to N7 of 5′-GMP. In contrast, large variations were observed over the pH* range 5–9. The pK_{a1} values calculated for the two isomers are 5.31 for **3** and 5.49 for **3***, which can be attributed to protonation of the phosphate group of 5′-GMP. The pK_{a2} values of 8.51 and 8.43 for **3** and **3***, respectively, can be associated with protonation of N1 of 5′-GMP. No variation of the H8 resonance at δ 8.10 (described above) was observed over the pH range 8–10, suggesting that **4** is an N1-bound adduct.

The pH titration of **3/3*** was also followed by ^{31}P NMR spectroscopy. A plot of chemical shift (δ) against pH for both chelate and dangling-arm phosphorus atoms showed identical profiles (Fig. 5b), from which pK_{a1} values of 5.29 and 5.46 for **3** and **3***, respectively, were calculated. These can be associated with the protonation of the phosphate group and agree well with the values above, derived from the ^1H NMR data.

The ^{31}P-{^1H} NMR spectra for the pH titrations also showed a number of additional peaks (collectively assigned to species **4**), in the ranges of δ 28.0 to δ 25.0 and δ −4.0 to δ −9.0. These correspond to the P atom within the chelate ring (P_a) and the P atom of the dangling arm (P_c), respectively, above pH* 6.5. Thus the ^{31}P-{^1H} NMR data are consistent with the ^1H NMR data described above, which indicated the formation of an N1-bound adduct.

A plot of the relative populations of all the species in solution, derived from the integration of the relevant peaks in the ^{31}P-{^1H} spectra, as a function of pH*, is shown in Fig. 6. Complex **4** became the dominant adduct above pH* 8.5. Species **4** appears to be derived from species **3**, since the amount of **3*** appears to remain constant over the measured pH range.

Effect of chloride ions. In all of the reactions of **1** with 5′-GMP, the presence of a small amount of unreacted **1** was always noted, even after the addition of two mole equivalents of 5′-GMP. The relative binding strengths of 5′-GMP and Cl^- were studied by a reverse titration of the 5′-GMP complex **3/3*** with chloride ions. Complex **3/3*** was prepared by precipitating all the chloride from complex **1** with $AgNO_3$ (to give complex **2**) prior to the addition of an equimolar amount of 5′-GMP. The resulting ^{31}P-{^1H} NMR spectrum showed formation of the two 5′-GMP adducts (**3** and **3***), but no signals for the ring-closed complex **2**. This solution of **3/3*** (20 mM, pH* 8.5) was titrated with chloride. The addition of increasing quantities of chloride ions resulted in increasing amounts of the ring-opened complex **1** (Fig. 7). With a 10-fold molar excess of chloride ions (200 mM) present, 50% of the bound 5′-GMP was displaced. These data suggest that 5′-GMP binds about 10 times more strongly than chloride.

Effect of temperature. Variable temperature ^1H and ^{31}P-{^1H} NMR experiments were carried out on **3/3*** at pH* 5.5 in order to detect possible chemical exchange between the major isomer **3** and minor isomer **3***. No coalescence of the H8 ^1H NMR signals was observed, even at 353 K. However, resonance broadening was significant, especially in the aromatic region of the ^1H NMR spectra. The ratio of the two isomers remained relatively constant over the temperature range 278–353 K. A significant increase in the amount of free 5′-GMP was observed at the expense of both adducts **3** and **3***. Twice as much free 5′-GMP was observed at 328 K compared with 278 K. The original ratios of free and bound forms of 5′-GMP were restored on returning the sample to ambient temperature. The corresponding ^{31}P-{^1H} NMR study revealed broadening of resonances assigned to the P-bound ring-opened ligand (P_c) with increasing temperature, whereas the resonances from the P in the P, N chelate ring (P_a) remained sharp with well resolved $^2J(^{31}P–^{31}P)$ couplings of 17 Hz. The amount of free 5′-GMP and free complex increased with increasing temperature, thereby confirming earlier observations that the dissociation of 5′-GMP was enhanced at elevated temperatures.

Exchange studies

Since the exchange processes were slow on the NMR timescale, ^1H 2-D-EXSY NMR spectroscopy was used to determine exchange rates. The effects of temperature (over the range 288–318 K) and of pH (over the range of 5.4–8.5) on the dynamics of the exchange process were studied under chloride-free conditions. A ^1H–^1H 2-D-EXSY NMR spectrum acquired for an equimolar mixture of **2** and 5′-GMP at pH* 5.4 (temperature = 298 K) is shown in Fig. 8a. The cross-peaks **c/c′** result from chemical exchange between the major and minor adducts, **3** and **3***. The presence of cross-peaks **a/a′** and **b/b′** indicate exchange between isomer **3** and 5′-GMP, and isomer **3*** and 5′-GMP. Spiking with excess 5′-GMP confirmed that the resonance at δ 8.10 corresponded to that of the H8 resonance of free 5′-GMP.

The exchange processes under these conditions (pH 5.4, 298 K) are described by Scheme 2 and rate constants for the exchange processes were determined to be: $k_1 = 0.05 \pm 0.01$ s^{-1}; $k_2 = 0.06 \pm 0.01$ s^{-1}; $k_3 = 0.07 \pm 0.01$ s^{-1}; $k_4 = 0.03 \pm 0.01$ s^{-1}; $k_5 = 0.09 \pm 0.01$ s^{-1}; $k_6 = 0.20 \pm 0.01$ s^{-1}. The formation of **3**

Table 5 ^{1}H NMR assignments for the sugar protons of 5′-GMP and isomeric GMP adducts **3** and **3***, (pH* 5.5, 298 K)

	δ (^{1}H)					
Adduct	H1′	H2′	H3′	H4′	H5′ or H5″	H5″ or H5′
3	5.930	5,028	4.586	4.498	4.169	4.120
3*	5.954	4.795	4.498	4.335	4.050	4.050
5′-GMP	5.933	4.716	4.528	4.446	4.184	4.081

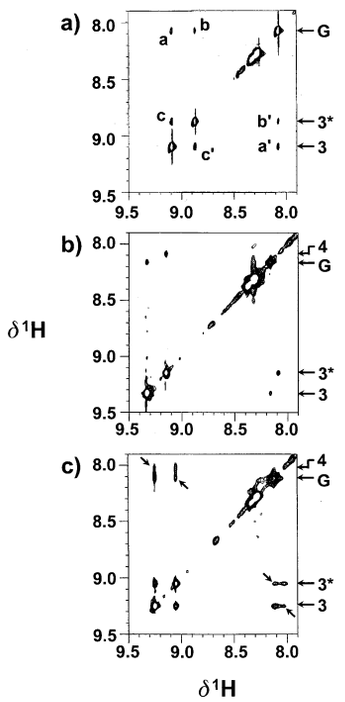

Fig. 8 600 MHz ^{1}H 2-D-EXSY NMR spectra of a solution of equimolar **2** and 5′-GMP in the region containing resonances for H8 of 5′-GMP. (a) pH* 5.4, 298 K; (b) pH* 8.5, 288 K; (c) pH* 8.5, 318 K; **G** = free 5′-GMP. **4** = N1 bound complex. Arrows in (c) indicate the presence of new exchange cross-peaks, which appear on raising the temperature of the sample at pH* 8.5.

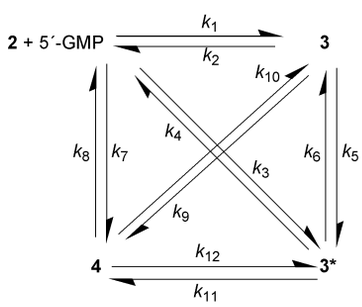

Scheme 2

from **2** and 5′-GMP therefore occurred at a similar rate to the dissociation process whereas the formation of **3*** from **2** and 5′-GMP occurred at twice the rate compared with dissociation of **3*** into **2** and 5′-GMP. The rate of conversion of **3*** to **3** is twice the rate of formation of **3*** from **3**.

The same mixture was also studied at pH* 8.5 over the temperature range 288–328 K. Two ^{1}H–^{1}H 2-D-EXSY data sets are presented for the sample at 288 K and 318 K (Fig. 8). The data show the presence of **4** in exchange with **3**/**3***. At low temperature (Fig. 8b) no conversion between **3** and **3*** is observed, as evidenced by the absence of an exchange cross-peak between the H8 resonances corresponding to **3** and **3***. The dominant exchange processes are between **3** and 5′-GMP and between **3*** and the new species **4**. The data suggest that exchange processes between **3** and **4** or between **3*** and 5′-GMP are absent. At higher temperature, the **3** to **3*** conversion becomes apparent, the data revealing a four-site exchange process as represented in Scheme 2. The interconversion rate between **3** and **3*** varied from 0.01 s^{-1} at 298 K to 0.55 s^{-1} at 328 K for the forward process, compared with variations from 0.04 s^{-1} at 298 K to 2.29 s^{-1} at 328 K for the reverse process.

^{1}H NMR assignments and nOes. In order to investigate further the nature of the complexes formed between **2** and 5′-GMP in solution, and to rationalise the observed exchange characteristics, 2-D ge-COSY45 and TOCSY data sets were acquired and analysed. The ^{1}H NMR resonance assignments are shown in Table 5. A number of through-space interactions were identified from NOESY data. In particular, strong nOes were observed between base H8 and sugar H2′ protons in both **3** and **3*** indicating a preferred sugar C2′-*endo* geometry. At 288 K, nOe and exchange cross-peaks were negative. As the temperature was raised, the nOes reduced in intensity compared with the exchange cross-peaks, which increased in size. At 308 K all nOes were close to zero. At temperatures above 308 K, the nOe cross-peaks were positive, while exchange cross-peaks remained negative. The nOes indicated a preferred *anti* orientation for the base moiety with respect to the sugar ring in each case.

Reaction of 1 with GMP analogues

Reactions were carried out between **1** and guanine derivatives differing either in the position of the phosphate group (*e.g.* 3′, 5′-cyclic GMP or 3′-GMP) or in the nature of the group attached to the base (*e.g.* 9-ethylguanine). The reactions were followed by 1-D ^{31}P-{^{1}H} NMR spectroscopy and the results are summarised in Table 4. Data for all of the adducts, recorded at pH* ≈5.0, were consistent with P in a P, N chelate ring, together with P *trans* to N7. The chemical shifts and coupling constants were similar to those for the 5′-GMP adduct. The major difference was that the **3**:**3*** isomer ratios were close to 1:1 for the 3′-GMP and 3′, 5′-cyclic-GMP adducts. In the case of 9-ethylguanine only a single adduct (complex **5**) was formed.

Molecular modelling

The force field reported previously,[20] and extended here to include phosphine ligands, accurately reproduced the structure of **1**. However, given the small data set used to derive the parameters for the phosphine moiety, the results should be taken as being more qualitative than quantitative. To complement the NMR and chemical studies described in previous sections, and to investigate the nature of the two isomers formed, molecular models of *cis*-[Pt(9-ethylguanine-N7)(Me_2N-$(CH_2)_2PPh_2$-*N*,*P*)($Me_2NH(CH_2)_2PPh_2$-*P*)]$^{3+}$ (**5**) and of *cis*-[Pt(5′-GMP-N7)($Me_2N(CH_2)_2PPh_2$-*N*,*P*)($Me_2NH(CH_2)_2PPh_2$-*P*)]$^{3+}$ (**3**/**3***) were built. Complex **1** is not chiral but when the chloro-ligand is replaced by an unsymmetrical ligand, such as 9-ethylguanine, enantiomers are generated, a consequence of the incoming ligand having a head-to-tail directionality. Thus two isomers are possible for **5**. One isomer has the guanine H8 and the ring-opened amino pendant arm of the ligand on the same side of the coordination plane (**5a** in Scheme 3). In the

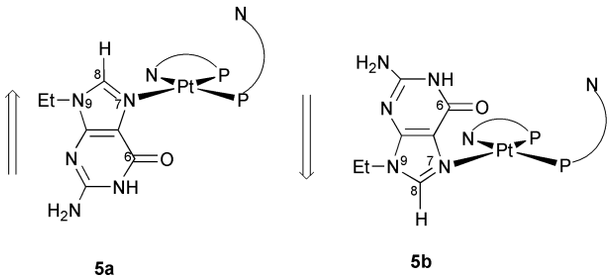

Scheme 3

Table 6 Strain energies

Compound	Isomer	Strain energy/ kJ mol^{-1}
5	**5a**	28.9
	5b	29.2
3/3*	**3a**	46.9
	3b	50.8
	3a*	46.8
	3b*	49.6

other isomer, the guanine H8 and the ring-opened amino pendant arm of the ligand are on opposite sides of the coordination plane (**5b** in Scheme 3). Molecular mechanics calculations show that isomer **5a** is preferred by about 0.3 kJ mol^{-1} over **5b** (Table 6).

When the incoming ligand is itself chiral, as is the case for 5′-GMP, diastereomers are generated and these give rise to the separate peaks observed in the NMR spectra of **3/3***. Four energetically distinct species are possible (Scheme 4), since there are two diastereomeric forms of each rotational isomer. The diastereomers have similar strain energies (Table 6), but in each case the rotational isomers **3a** and **3a*** (Scheme 4) with the guanine H8 located on the same side of the coordination plane as the amino group of the ring-opened ligand are preferred by 3–4 kJ mol^{-1} over **3b** and **3b*** (Table 6). Barriers to rotation about Pt–P (ring-opened) and Pt–N7 (guanine) bonds were estimated using constrained refinement to step through the rotation process. For the former, the barrier is approximately 55 kJ mol^{-1} and for the latter it is greater than 100 kJ mol^{-1}. Thus, rotation about the Pt–P bond is a facile process that will occur at a significant rate but rotation about Pt–N7 is impeded by interactions between the guanine and the coordination plane and will occur only at elevated temperatures.

Discussion

X-Ray structure of 1

The protonated, ring-opened complex *cis*-[Pt($Me_2N(CH_2)_2$-PPh_2-*N*,*P*)Cl($Me_2NH(CH_2)_2PPh_2$-*P*)]$(NO_3)_2$·1.5H_2O, **1a**, has a long Pt–N bond relative to those in previously reported aminophosphine complexes, which incorporated less hindered nitrogen centres.[24] The weakening of the Pt–N bond in **1** can therefore be ascribed partly to steric effects.[30] Under conditions of low pH or in the presence of nucleophiles (such as chloride ions), one of the Pt–N bonds in the ring-closed complex, **2**, is labile and susceptible to cleavage. In contrast, it is difficult to ring-open the unsubstituted complex *cis*-[Pt($H_2N(CH_2)_2PPh_2$-*P*,*N*)$_2$]Cl_2 even at much lower pH* values.[24] Therefore under physiological conditions one of the 5-membered chelate rings of **2** can open, thereby providing a site for reaction with biomolecules such as DNA.

Dynamics of chelate ring-opening and -closing

The assignments of ^{31}P NMR signals for the chelate ring-closed complex, **2**, and ring-opened complex **1** were based on chemical shifts and coupling constants. Under the experimental conditions used, no aquated adducts were observed. Resonance broadening observed in the 1-D ^{31}P NMR spectra suggested the existence of an exchange process between **1** and **2**. 2-D ^{31}P EXSY NMR, variable temperature NMR studies and NMR simulations, confirmed that this was the case. The equilibrium is dependent on chloride ion concentration and pH. The dynamic nature of this chelate ring-opening and -closing process was investigated by 2-D ^{31}P–^{31}P EXSY NMR spectroscopy. Short mixing times (< 10 ms) and long relaxation delays (> 10 s) were required in order that consistent exchange rate data were obtained from the EXSY data sets. This was a reflection of the rates of exchange which were found to vary significantly, but were never less than 9 s^{-1} for either opening or closing rates, and often much faster. 2-D EXSY NMR has been extensively applied to the analysis of dynamic equilibria, which are slow on the NMR timescale.[31,32] The extraction of rate constants from such data, carried out either by initial rate, iterative or direct matrix transformation analysis, provides details of the thermodynamics governing dynamic equilibria.

The pH dependence of the chelate ring-opening and -closing process is significant in physiological terms. At high pH > 7.5 the rate of ring-closure is high whereas lowering the pH to less

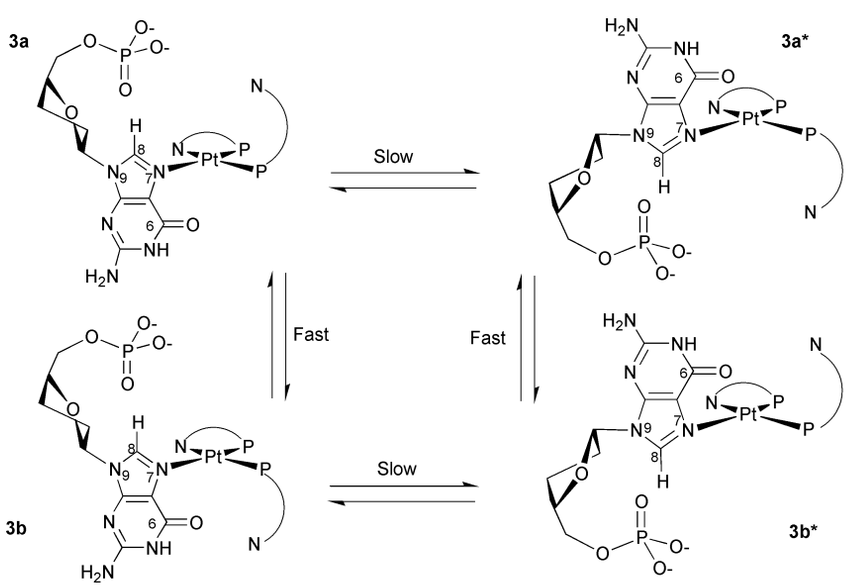

Scheme 4

than 5.5 causes the ring-closing rate to tend towards zero (Fig. 3). Under such conditions the ring-opened form, **1**, dominates. The implication for tumor cells, which often experience low associated pH conditions,[33] will be for the complex to react more readily at tumor cell sites as a result of the available binding site on the metal centre. The ring-closed form, present at higher pH and being cationic and lipophilic, is likely to bind to mitochondrial membranes and disrupt membrane potentials.[2] Chloride ions also significantly affect the position of the equilibrium. The rate of ring-opening increases with increasing chloride ion concentration, consistent with a bimolecular process. The increase in the rate of ring-closure is consistent with an increase in the amount of ring-opened complex as the chloride concentration increases. The proportion of ring-closed species is likely to increase inside cells where the chloride concentration (*ca*. 4 mM) is usually lower than outside cells (*ca*. 104 mM).

Activation parameters. Studies of the exchange rates at various pH values and temperatures enabled activation parameters to be obtained. The negative entropies of activation for this equilibrium, $\Delta S^{\ddagger}$ (Table 3) are features normally associated with an intra-molecular process.[34–36] This implies that the two-site exchange process, involving chelate ring-opening and ring-closing, is governed by an associative mechanism, involving a 5-coordinate intermediate. Formation of the Pt–Cl bond and dissociation of the Pt–N bond would then occur in a concerted fashion, with the incoming nucleophile approaching from above or below the Pt square plane. Examination of models based on the X-ray crystal structure of **1a** show that this is the only feasible mode of approach for incoming nucleophiles. In the absence of any chloride ions, chelate ring-opening occurs only at very low pH values (< 2).[24]

Structure and dynamics of the 5′-GMP adducts of 2

The reaction of $[Pt(Me_2N(CH_2)_2PPh_2\text{-}P,N)_2]^{2+}$ (**2**) with 5′-GMP was rapid, being essentially complete by the time the first NMR spectrum had been acquired. This is in contrast to reactions of platinum(II) ammine complexes with 5′-GMP, which are slow, but similar in rate to palladium(II) complexes.[37] The high reactivity of platinum(II) in **2** can be attributed to the high *trans* effect of the phosphorus atom. The binding of 5′-GMP through N7 was established on the basis of the shift of the H8 NMR resonance of the bound 5′-GMP compared with the free form, when studied over a wide range of pH* values (Fig. 6). ^1J(P, Pt) coupling constants of 3203 and 3468 Hz, are typical of ^{31}P *trans* to N,[8,26] *trans* to N within the chelate ring and to N7 in the purine ring, respectively. The major site of attack by platinum am(m)ine anti-cancer complexes is N7 of guanine, which is readily accessible in the major groove of duplex DNA and is the strongest electron donor of the four bases.[38] The primary binding site for **2** under acidic or neutral conditions is the N7 position on 5′-GMP. However, under basic conditions N1 appears to bind. Complexes containing Pt–N1 binding have been prepared previously[39] but under physiological conditions N1 of guanine in duplex DNA is involved in Watson–Crick base pairing. This position is therefore not available for metal binding. Metal ion binding at the N7 position acidifies the proton at N1 by about 1.5–2 log units,[40] thus rendering the N1 site more accessible to platinum. The presence of an intermediate binuclear species, in which platinum is bound simultaneously to both N1 and N7, is also possible. At pH* 5–6 a migration of $[Pt(II)(dien)]^{2+}$ from inosine N7 to N1 occurs *via* slow build-up and loss of a binuclear intermediate.[41] The N3 atom of guanine is not usually a strong Pt-binding site, because it is in a sterically-crowded position. Simultaneous binding of platinum(II) to three different sites (N7, N1, N3) of a guanine nucleobase has been reported by Lippert *et al.*[42] Thus binding at the N3 site cannot be excluded in the present study. More peaks were present in the ^{31}P NMR spectrum than can be accounted for by binding at the N7 and N1 positions alone.

For **3/3***, four energetically distinct species are possible, since there are two diastereomeric forms of each rotamer (Scheme 4). Four distinct resonances would be anticipated from the 4 diastereomers, but only two isomers in a 3:1 ratio (pH* 5.5) were observed experimentally, as was indicated by the appearance of two H8 signals and two sets of resonances in the ^{1}H and ^{31}P NMR spectra. Two conditions could give rise to this observation: i) only one set of the two possible pairs of rotamers (**3a** and **3b** or **3a*** and **3b***, Scheme 4) is favoured, or ii) rapid interconversion between diastereomers in each set of rotational isomers occurs, giving rise to two sets of averaged NMR signals corresponding to **3** and **3***. The latter seems to be the case as suggested by the molecular mechanics studies (*vide infra*). The major isomer was most favoured in the pH range where the phosphate group was largely deprotonated. The phosphate group may be involved in H-bonding with the amine group of the dangling arm, which could favour the stabilisation of the major isomer. This was further elaborated by molecular modelling studies (see the section on molecular modelling). Studies with both 3′-GMP and 3′, 5′-cyclic GMP showed changes in the isomer ratio, with each being present in equal amounts in each of these cases. This supports the assertion that the position of the phosphate group on the chiral sugar moiety of GMP plays a prominent role in influencing the orientation of the purine ring in relation to the metal centre. The NMR spectrum of the 9-ethylguanine adduct, **5** (which lacks the chiral sugar) contained only a single H8 resonance in the ^{1}H NMR spectrum, and gave rise to only one set of ^{31}P NMR resonances.

Exchange rate analysis

At pH* 5.4 it was clear that a classical three-site exchange process existed between **3**, **3*** and **2** + 5′-GMP in the absence of chloride ions. The exchange processes were shown to be slow with conversion lifetimes in the range 5–50 s. At pH* 8.5 the exchange system was altered by the presence of the additional species **4**. At 288 K, no interconversion occurred between **3** and **3***. However, **3** was in exchange specifically with **2** + 5′-GMP (denoted by the resonance **G** in Fig. 8c, corresponding to free 5′-GMP) and **3*** was in exchange specifically with **4**. With increasing temperature, exchange between **3** and **3*** was observed together with additional exchange processes, namely **3** to **4** and **3*** to **2** + 5′-GMP, processes which were absent at lower temperatures.

The NMR data show that once conversion between **3** and **3*** becomes more facile, conversion between **3** and **4** and between **3*** and **2** + 5′-GMP can be observed, without the need for conversion between **4** and **2** + 5′-GMP. Thus it appears that formation of **4** from **2** + 5′-GMP cannot occur directly at this pH, but must go *via* **3/3***. This suggests that pre-binding at N7 is required to lower the pK_a value of N1 (pK_a of N1 is lowered by *ca*. 1.2 log units in **3/3***) so that formation of **4** becomes favourable through this route.

Effect of chloride ions. In platinum(II) am(m)ine complexes nucleobase binding is stable due to the inertness and high thermodynamic stability of the Pt–N bonds.[5] The facile displacement of 5′-GMP in **3/3*** by chloride is unusual in comparison with platinum(II) am(m)ine complexes. This is probably due to the relatively strong *trans* effect of the coordinated phosphino group. Normally the displacement of nucleobases from platinum requires strong nucleophiles such as CN^- and sulfur ligands.[43] However, in a few cases migration of coordinated platinum(II) from one nucleobase to another has been reported in both single-stranded[44,45] and double-stranded oligonucleotides.[45,46] The rates of displacement of guanine from *cis*-$[Pt(NH_3)_2(guanine\text{-}N7)_2]^{2+}$ by thiourea and other sulfur-containing nucleophiles have been studied by ^{13}C NMR

spectroscopy and were found to be relatively slow (the rate of displacement at 316 K was 1.5×10^{-5} s^{-1} for thiourea).[47] For [Pt(dien)(guanine-N7)]$^{2+}$, the displacement of the coordinated nucleobase follows an associative mechanism in both neutral and acidic aqueous solution, as do reactions with thiourea in neutral solutions.[48]

Molecular modelling. The modelling studies using the 9-ethylguanine adduct of **1,** *cis*-[Pt(9-ethylguanine-N7)(Me_2N-$(CH_2)_2PPh_2$-*N*,*P*)($Me_2NH(CH_2)_2PPh_2$-*P*)]$^{3+}$, **5**, revealed that isomer **5a** is preferred over isomer **5b** by *ca.* 0.3 kJ mol^{-1}. Isomer **5a** is arranged in such a way that the purine moiety is orientated with the H8 of the guanine on the same side of the coordination plane as the amino pendant arm of the ligand in contrast to isomer **5b**, in which the purine moiety has the opposite orientation. This preference is in spite of the fact that the exocyclic O6 (guanine) is capable of forming a hydrogen bond with the amino group of the pendant arm. These isomers can be inter-converted in two ways. The first way is by rotation about the Pt–P (ring-opened) bond or by rotation about the Pt–N7 (guanine) bond. The second way is by the dissociation of the 9-ethylguanine ligand, followed by closure of the aminophosphine chelate ring, opening of the other chelate ring and coordination of the 9-ethylguanine in the same orientation with respect to the coordination plane. A further stabilising feature could be π–π stacking interactions between the 6-membered aromatic ring of the purine moiety and one of the phenyl groups. In the case of the 5′-GMP adducts, which have a chiral sugar, diastereomers are generated. The preference for the formation of isomers **3a** and **3a*** by 3–4 kJ mol^{-1} over **3b** and **3b*** is consistent with the result for the 9-ethylguanine adduct, which revealed an inherent preference for **5a**. Hydrogen bonds are possible for both rotational isomers, these being between the phosphate and amino groups in the case of **3a** and **3a*** and between guanine O6 and the amino group for **3b** and **3b***. In modelling these hydrogen bonds, no account was taken of the differences in their energies. However, the hydrogen bond between the protonated dangling arm amino and phosphate groups is likely to be more stable since both groups are charged. Therefore, the preference for **3a** and **3a*** is likely to be underestimated. Intramolecular hydrogen bonding between the NH of *cis*-PtA_2 and the phosphate backbone of DNA is believed to influence the structure of the Pt–DNA adduct and hence the activity of the platinum complex.[27,49] Recent X-ray crystallographic studies of a 16-base-pair DNA duplex containing a site-specific *cis*-[$Pt(NH_3)_2${d(GpG)-N7(1),-N7(2)}] have shown that the NH_3 group is within 3.2 Å of the phosphate oxygen atom, which is close enough to participate in hydrogen bonding.[50] Furthermore, in a DNA dodecamer containing a 1,2-intrastrand d(GpG)-cisplatin adduct, one of the ammine ligands bound to platinum is H-bonded to a phosphate oxygen.[51] In BipPt(guanine-N7)$_2$ (Bip = 2,2′-bipiperidine) the rotamer distribution was found to be influenced by phosphate–NH(Bip) hydrogen bonds.[52]

Inter-conversion between rotamers can occur *via* two processes. The first of these is by simultaneous rotation about the Pt–P (ring-opened) and Pt–N7 (guanine) bonds. The second is by the dissociation of 5′-GMP, for inter-converting the enantiomers of **3**. The latter dissociative process seems to be more likely in view of the positive $\Delta S^{\ddagger}$ values obtained for the inter-conversion between the major and minor isomers.

Conclusions

The aminophosphine complex, *cis*-[$Pt(Me_2N(CH_2)_2PPh_2$-*P*,*N*)$_2$]Cl_2, **2**, has been shown by ^{1}H and ^{31}P NMR studies to undergo reversible chelate ring-opening reactions in aqueous solution. The rate for this process varies significantly with pH, chloride ion concentration and temperature and was found to be governed by an associative mechanism, involving a 5-coordinate intermediate. ^{31}P-2-D EXSY NMR spectroscopic studies showed that the rate of ring-opening is accelerated at low pH and high chloride ion concentration. The X-ray crystal structure of *cis*-[$Pt(Me_2N(CH_2)_2PPh_2$-*N*,*P*)$Cl(Me_2NH(CH_2)_2$-PPh_2-*P*)]$(NO_3)_2 \cdot 1.5H_2O$, **1a**, was determined and the complex has a relatively long Pt–N bond (2.147 Å). The nucleotide 5′-GMP binds rapidly and reversibly to complex **2** *via* N7 which induces aminophosphine chelate ring-opening. Above pH* 8.2, the predominant species appear to be non N7-bound adducts. The facile displacement of 5′-GMP in *cis*-[Pt(5′-GMP-*N7*)-($Me_2N(CH_2)_2PPh_2$-*N*,*P*)($Me_2NH(CH_2)_2PPh_2$-*P*)]$^{3+}$ (**3/3***) by chloride is unusual in comparison with platinum(II) am(m)ine complexes. ^{1}H 2D-EXSY NMR studies reveal a slow exchange process between Pt-bound and free-5′-GMP together with the existence of two isomers. The two isomers observed by NMR (**3** and **3***) can be formulated as diastereomers, which essentially differ in the orientation of the plane of the purine residue. In one isomer the O6 of the guanine is above, and in the other isomer, below the platinum plane. Molecular mechanics calculations suggest that these nucleotide adducts are stabilized by H-bonding between the dangling arm amino group and the 5′-phosphate of the nucleotide.

The features described here have at least two significant biological consequences for the design and action of Pt-based drugs. Firstly, the reversible binding of platinum(II) aminophosphine complexes to 5′-GMP with lifetimes in the range 5–50 s is in marked contrast to the behaviour of cisplatin binding. Binding of cisplatin to DNA is usually non-reversible and may be kinetically driven. A platinum(II) aminophosphine complex, in contrast, is likely to be mobile on DNA and to establish an equilibrium in which it is bound to the most thermodynamically favoured site. The second biological consequence is a dual mode of action. The ring-closed form of the aminophosphine complex is formed in environments of low chloride concentration and therefore antimitochondrial activity could form part of its mode of action. However, increasing the bulk of the substituents on N can hinder ring closure, a situation which may favour direct coordination to DNA bases.[24]

Acknowledgements

We thank the BBSRC and EPSRC for support and Dr. Keith Orrell, University of Exeter for the D2DNMR software package. We have benefited from stimulating discussions with members of the EC COST Action D8.

References

1 A. Habtemariam and P. J. Sadler, *Chem. Commun.*, 1996, 1785.
2 S. J. Berners-Price, R. J. Bowen, M. J. McKeage, P. Galettis and P. C. Healy, *Coord. Chem. Rev.*, 1999, **185**, 823 and references therein; S. J. Berners-Price, R. J. Bowen, M. J. McKeage, P. Galettis, L. Ding, B. C. Baguley and W. J. Brouwer, *Inorg. Biochem.*, 1997, **67**, 154.
3 K. Neplechová, J. Kašpárková, O. Vrána, O. Novákoaá, A. Habtemariam, B. Watchman, P. J. Sadler and V. Brabec, *Mol. Pharmacol.*, 1999, **56**, 20.
4 N. Margiotta, A. Habtemariam and P. J. Sadler, *Angew. Chem.*, *Int. Ed. Engl.*, 1997, **36**, 1185.
5 F. Basolo and R. G. Pearson, *Mechanisms of Inorganic Reactions*, Wiley, New York, 1967, Ch. 5.
6 R. G. Wilkins, *Kinetics and Mechanism of Reactions of Transition Metal Complexes*, VCH, Weinheim, 1991, Ch. 4.
7 T. W. Hambley, *Inorg. Chem.*, 1988, **27**, 1073.
8 G. K. Anderson and R. Kumar, *Inorg. Chem.*, 1984, **23**, 4064.
9 KALEIDAGRAPH, version 3.09, Synergy Software, Reading, PA, 1997.
10 X-SHAPE, *Crystal Optimisation for Absorption Correction*, Stoë and Cie, Darmstadt, Germany, 1996.
11 W. Clegg, *Acta Crystallogr.*, *Sect. A*, 1981, **37**, 22.
12 P. T. Beurskens, G. Beurskens, W. P. Bosman, R. de Gelder, S. Garcìa-Granda, R. O. Gould, R. Israël and J. M. M. Smits, DIRDIF-96, Crystallography Laboratory, University of Nijmigen, The Netherlands, 1996.

13 G. M. Sheldrick, SHELXL-97, University of Göttingen, Germany, 1997.
14 D. J. States, R. A. Haberkorn and D. J. Ruben, *J. Magn. Reson.*, 1982, **48**, 286.
15 E. W. Abel, T. P. J. Coston, K. G. Orrell, V. Sîk and D. Stephenson, *J. Magn. Reson.*, 1986, **70**, 34.
16 gNMR, version 3.6, Cherwell Scientific Publishing Limited, Oxford, 1995.
17 J.-J. Delpuech, in *Dynamics of Solutions and Fluid Mixtures by NMR*, ed. J.-J. Delpuech, John Wiley & Son, Chichester, 1995, p. 112.
18 HYPERCHEM, Hypercube Inc., Ontario, Canada, 1995.
19 T. W. Hambley and P. Comba, MOMECSGI, A Strain Energy Minimisation Package Adapted to HyperChem., University of Sydney, 1994.
20 T. W. Hambley, *Inorg. Chem.*, 1991, **30**, 937; E. C. L. Ling, G. W. Allen and T. W. Hambley, *J. Chem. Soc.*, *Dalton Trans.*, 1993, 3705; S. J. Weiner, P. A. Kollman, D. A. Case, U. C. Singh, C. Ghio, G. Alagona, S. Profeta Jr. and P. Weiner, *J. Am. Chem. Soc.*, 1984, **106**, 765; T. W. Hambley, *Inorg. Chem.*, 1998, **37**, 3767.
21 T. W. Hambley, *J. Comput. Chem.*, 1988, **8**, 651.
22 G. J. Palenik and T. J. Giordano, *J. Chem. Soc.*, *Dalton Trans.*, 1987, 1175.
23 A. G. Orpen, L. Brammer, F. H. Allen, O. Kennard, D. J. Watson and R. Taylor, *J. Chem. Soc.*, *Dalton Trans.*, 1987, S1.
24 A. Habtemarian, B. Watchman, R. Palmer, B. Potter, S. Parsons, A. Parkin and P. J. Sadler, *J. Chem. Soc.*, *Dalton Trans.*, in press.
25 P. E. Garou, *Chem. Rev.*, 1981, **81**, 229.
26 P. S. Pregosin, in *Phosphorus-31 NMR Spectroscopy in Stereochemical Analysis*, eds. J. G. Verkade and L. D. Louis, VCH, New York, 1987, p. 465.
27 S. J. Berners-Price, U. Frey, J. D. Ranford and P. J. Sadler, *J. Am. Chem. Soc.*, 1993, **115**, 8649.
28 K. H. Scheller, V. Scheller-Krattinger, R. B. Martin, *J. Am. Chem. Soc.*, 1981, **103**, 6833.
29 F. J. Dijt, G. W. Canters, J. H. J. den Hartog, A. T. M. Marcelis and J. Reedijk, *J. Am. Chem. Soc.*, 1984, **106**, 3644.
30 A. Tongi and L. M. Venanzi, *Angew. Chem.*, *Int. Ed. Engl.*, 1994, **33**, 497.
31 K. G. Orrell, in *Encyclopedia of Nuclear Magnetic Resonance*, eds. D. M. L. Grant and R. K. Harris, Wiley, Chichester, UK, 1996, vol. 8, pp. 4850–4857.
32 V. Jacques and J. F. Desreux, *Inorg. Chem.*, 1994, **33**, 4048.
33 G. Lamm and G. R. Pack, *Proc. Natl. Acad. Sci. USA*, 1990, **87**, 9033.
34 K. G. Orrell, A. G. Osborne, V. Šik, M. Webba da Silva, M. B. Hursthouse, D. E. Hibbs, K. M. Abdul Malik and N. G. Vassilev, *Organomet. Chem.*, 1998, **555**, 35.
35 P. Fisher and A. Fettig, *Magn. Reson. Chem.*, 1997, **35**, 839.
36 A. Gelling, D. R. Noble, K. G. Orrell, A. G. Osborne and V. Šik, *J. Chem. Soc.*, *Dalton Trans.*, 1996, 3064.
37 R. B. Martin, in *Cisplatin-Chemistry and Biochemistry of a Leading Anticancer Drug*, ed. B. Lippert, Verlag, Zürich, 1999, pp. 183–205.
38 A. Pullman and B. Pullman, *Q. Rev. Biophys.*, 1981, **14**, 289; A. L. Pinto and S. J. Lippard, *Biophys. Acta*, 1985, **780**, 167; I. Saito, M. Takayama, H. Sugiyama, K. Nakatani, A. Tsuchida and M. Yamamoto, *J. Am. Chem. Soc.*, 1995, **117**, 6406.
39 G. Frommer, I. Mutikainen, F. J. Pesch, E. C. Hillgeris, H. Preut and B. Lippert, *Inorg. Chem.*, 1992, **31**, 2429.
40 K. H. Scheller, V. Scheller-Krattinger and R. B. Martin, *J. Am. Chem. Soc.*, 1981, **103**, 6833; J. H. J. den Hartog, M. L. Salm and J. Reedijk, *Inorg. Chem.*, 1984, **23**, 2001.
41 R. B. Martin, in *Platinum*, *Gold and Other Metal Chemotherapeutic Agents: Chemistry and Biochemistry*, ed. S. J. Lippard, American Chemical Society, Washington, DC, 1983, ACS Symposium Series vol. 209, p. 231.
42 G. Raudaschl-Sieber, H. Schollhorn, U. Thewalt and B. Lippert, *J. Am. Chem. Soc.*, 1985, **107**, 3591.
43 B. Lippert, in *Progress in Inorganic Chemistry*, ed. S. J. Lippard, Wiley, New York, 1989, vol. 37, pp. 1–97.
44 S. L. Bruhn, J. H. Toney and S. J. Lippard, in *Progress in Inorganic Chemistry*, ed. S. J. Lippard, Wiley, New York, 1990, Vol. 38, pp. 477–516.
45 M. Boudvillain, R. Dalbiès and M. Leng, in *Metal Ions in Biological Systems*, eds. A. Sigel and H. Sigel, Marcel Dekker, New York, 1996, vol. 33, pp. 87–103.
46 D. Yang, S. S. G. E. van Boom, J. Reedijk, J. H. van Boom and A. H. J. Wang, *Biochemistry*, 1995, **34**, 12912.
47 J. A. Beaty and M. M. Jones, *Inorg. Chem.*, 1992, **31**, 2547.
48 M. Mikola, K. D. Kilka, A. Hakala and J. Arpalahti, *Inorg. Chem.*, 1999, **38**, 571.
49 Z. Guo, P. J. Sadler and E. Zang, *Chem. Commun.*, 1997, 27; S. J. Berners-Price, J. D. Ranford and P. J. Sadler, *Inorg. Chem.*, 1994, **33**, 5842; S. J. Berners-Price, T. A. Frenkiel, J. D. Ranford and P. J. Sadler, *J. Chem. Soc.*, *Dalton Trans.*, 1992, 2137.
50 E. R. Jamieson and S. J. Lippard, *Chem. Rev.*, 1999, **99**, 2467.
51 P. M. Takahara, C. A. Frederick and S. J. Lippard, *Nature*, 1995, **377**, 649; P. M. Takahara, C. A. Frederick and S. J. Lippard, *J. Am. Chem. Soc.*, 1996, **118**, 12309.
52 S. O. Ano, F. A. Intini, G. Natile and L. G. Marzilli, *Inorg. Chem.*, 1999, **38**, 2989.